An Atrial Fibrillation Detection Strategy in Dynamic ECGs With Significant Individual Differences

Caiyun Ma, *Graduate Student Member, IEEE*, Xi Long, *Senior Member, IEEE*, Weijie Sheng, Rik Vullings, *Senior Member, IEEE*, Meicheng Yang, Lina Zhao, Ronald M. Aarts, *Fellow, IEEE*, Jianqing Li, and Chengyu Liu, *Senior Member, IEEE*

***Abstract*— Atrial fibrillation (AF) is an insidious disease. Many long-term wearable electrocardiogram (ECG) monitoring devices have been used to monitor AF. The accuracy of detectors used to classify AF/sinus rhythm is already very high on the public database. Due to the significant individual differences and interference from other arrhythmias (e.g., premature beats), the performance of the developed AF detectors can degrade when tested on wearable ECGs. To tackle this, we proposed to use a domain-adversarial (DA) learning strategy to minimize feature distribution between the annotated public ECG database (the MIT-BIH AF database) and unlabeled dynamic ECG recordings to improve AF recognition accuracy. DA algorithms based on the shifted window transformer (DA-ST) and residual neural network (DA-RN) were proposed and validated on the 2021 China Physiological Signal Challenge (CPSC) database including four datasets. The accuracies were 93.85%, 89.78%, 91.93%, and 87.35% on the four datasets when using DA-ST. The corresponding results were 96.67%, 92.25%, 90.58%, and 89.46% when utilizing DA-RN. Importantly, these results demonstrated superior performance compared to the results obtained without DA. The proposed method was validated on 12 wearable long-term recordings, consisting of four recordings with premature beats, four recordings of AF with premature beats, two recordings of sinus rhythms, and two recordings of AF. The average results were 98.67% (DA-ST) and 97.89% (DA-RN), proving that the proposed method could provide reliable AF detection for dynamic ECG recordings with significant individual differences.**

***Index Terms*— Atrial fibrillation (AF), domain-adversarial network (DAN), dynamic electrocardiogram (ECGs), ECG, residual neural network (ResNet), shifted window transformer (Swin-Transformer).**

Manuscript received 25 June 2023; revised 4 September 2023; accepted 5 November 2023. Date of publication 28 November 2023; date of current version 3 January 2024. This work was supported in part by the National Natural Science Foundation of China under Grant 62171123, Grant 62071241, Grant 62201144, and Grant 62211530112; in part by the Natural Science Foundation of Jiangsu Province under Grant BK20192004; and in part by the Postgraduate Research and Practice Innovation Program of Jiangsu Province under Grant KYCX21_0089. The Associate Editor coordinating the review process was Dr. Boby George. *(Corresponding author: Chengyu Liu.)*

Caiyun Ma, Meicheng Yang, Lina Zhao, Jianqing Li, and Chengyu Liu are with the State Key Laboratory of Bioelectronics, School of Instrument Science and Engineering, Southeast University, Nanjing 211189, China (e-mail: caiyun@seu.edu.cn; meicheng@seu.edu.cn; zhaolina0808@126.com; ljq@seu.edu.cn; chengyu@seu.edu.cn).

Xi Long, Rik Vullings, and Ronald M. Aarts are with the Department of Electrical Engineering, Eindhoven University of Technology, 5612 AZ Eindhoven, The Netherlands (e-mail: x.long@tue.nl; r.vullings@tue.nl; r.m.aarts@tue.nl).

Weijie Sheng is with the School of Information Engineering, Yangzhou University, Yangzhou 225012, China (e-mail: wjsheng@yzu.edu.cn).

Digital Object Identifier 10.1109/TIM.2023.3335526

I. Introduction

Atrial fibrillation (AF) is an insidious disease related to high mortality and morbidity of many cardiovascular diseases, mainly occurring among the elderly [1]. The initial stage of AF is asymptomatic and usually presents as paroxysmal attacks. Its prevalence is increasing year by year [2]. The 2020 European Society of Cardiology (ESC) guidelines for the diagnosis and management of AF recommend AF screening for individuals over 65 years or with other symptoms indicating an increased risk of stroke [3]. Early screening at home is crucial for effective AF management. Additionally, monitoring AF frequency and duration is essential for developing surgical and treatment strategies [4], as it can significantly reduce the postoperative recurrence of AF [5].

Continuous monitoring of AF typically involves the use of a photoplethysmograph (PPG) and a wearable electrocardiogram (ECG) during daily life [6]. The PPG signal can be used as a prescreening tool to identify AF by rhythm, while the ECG is a powerful tool for monitoring the occurrence, maintenance, and termination of AF in clinical practice. AF can be identified on the ECG by the absence of P waves and an irregular RR interval. The AF detection rate from a 12-lead Holter monitor is around 16% [7], but studies have shown that longer monitoring periods, such as 48 or 72 h, can increase the detection rate of paroxysmal AF [8]. Wearable ECG monitoring devices allow for real-time continuous monitoring of patients' ECGs, which can greatly aid in the detection of AF. However, the abundance of unlabeled ECG data from continuous monitoring can create a significant burden for doctors attempting to diagnose AF. As a result, automatic diagnosis algorithms are needed to assist in the detection and diagnosis of AF.

AF analysis methods can be divided into three categories, shown in Table I. The first is analyzing the ECG characteristics during AF, including the RR interval analysis [9] and P-wave or F-wave features analysis [10]. The RR interval analysis used for AF detection includes the variability analysis of the instantaneous heart rates [11] and entropy features [12], such as sample entropy (SampEn), coefficient of SampEn, fuzzy

TABLE I
AF ANALYSIS METHODS

Methods	Detail
AF analysis based on Features	RR interval features analysis
	P-wave or F-wave features analysis
AF detection based on machine learning	RR interval features+machine learning (SVM, KNN, RF, etc)
	RR interval+P-wave or F-wave features +machine learning (SVM, KNN, RF, etc)
AF detection based on deep learning	ECG waves+deep learning (CNN, LSTM)
	ECG waves+TF analysis+2-D CNN

SVM: support vector machine, KNN: K-nearest neighbors, RF: random forest, CNN: convolutional neural network, LSTM: long-short term memory, TF: time-frequency.

measure entropy, normalized fuzzy measure entropy, etc. P-wave or F-wave features analysis is judging the presence of F waves or the absence of P waves, including detectors based on P-wave and F-waves [13], [14], wavelet entropy [15], relative wavelet energy [16], etc. The second is AF detectors that are based on machine learning and RR interval and P wave features. With the emergence of deep learning, several deep learning-based models have been proposed for AF detection on the PhysioNet/Computing in Cardiology (CinC) Challenge 2017 [17] which is the third AF detection method. Luo et al. [18] combined time-frequency analysis and 2-D convolutional neural network (CNN) to train an AF detector. Zhang et al. [19] used CNN or long short-term memory (LSTM) to detect AF. Currently, AF detection has matured significantly on open databases.

The ECG recordings are subject to interpersonal differences from the different individuals and wave differences measured from different monitoring devices. The poor generalization capability can be inevitable when tested on dynamic ECGs which limits the developed AF detectors to be robustly used in dynamic monitoring situations. The accuracy of the AF detector developed by Anderson et al. [20] dropped by about 10% on the independent dataset. The accuracy of the AF detector from Chang et al. [21] dropped by about 15% and 23% on two separate data. In our previous work [22], the AF detector proposed by Zhang et al. [23] is trained on the MIT-BIH AF database, and achieved a specificity of 77.75% and 65.85%, respectively, on the dataset1 and dataset2 from CPSC2021. The AF classifier presented by Maknickas and Maknickas [24] is also trained on MIT-BIH AF database, achieved results of 92.59% and 85.38% on the dataset1 and dataset2 from CPSC2021.

The common methods to improve model generalization ability is to pretrain the AF detection model on the open database and use part of the ECGs and labels from test data for fine-tuning the pretrained model. However, manual labeling of ECGs used for fine-tuning is still required, which can be a tedious task for long-term recordings with significant personalization differences. If the difference between the data distribution of unlabeled dynamic data and the labeled public database is minimized, the detection accuracy of the developed AF detectors on dynamic ECGs can be improved. Aligning labeled ECGs and unlabeled ECGs at the feature distribution without manual labeling of new data is a suitable method for recordings from dynamic continuous ECG monitoring. This approach can effectively improve the accuracy of AF detection models, while reducing the amount of manual labeling required for developing these models. It has the potential to help researchers and developers more efficiently and effectively develop accurate AF detection models for dynamic ECGs, which can have significant clinical implications for the diagnosis and treatment of AF.

Therefore, we proposed an improved AF detection method to align the feature distribution of open database ECGs and unlabeled dynamic ECGs. Two feature extractors are used: the shifted window transformer (Swin-Transformer) [25] and the residual neural network (ResNet) [26]. The Swin-Transformer uses self-attention based on moving windows and can utilize local prior knowledge to obtain features of different sizes, achieving superior results in various visual tasks. In this work, the Swin-Transformer is used to detect AF. The ResNet is used for automatic diagnosis of 12-lead ECG and has achieved good performance [26]. In this study, the ResNet is employed to detect AF from single-lead ECG. Additionally, domain-adversarial (DA) learning [27] is a representative method of adversarial transfer learning methods. We used the DA network (DAN) to reduce the feature distribution of open database ECGs and unlabeled dynamic ECGs. It is our hypothesis that the proposed method can improve the detection accuracy of AF from dynamic ECG recordings.

In this work, we combined the Swin-Transformer and the ResNet with the DAN respectively to address the impact of significant individual differences in ECG recordings. The algorithms were verified on the annotated public database: MIT-BIH AF database [28], [29] and the 4th China Physiological Signal Challenge (CPSC2021) database with individual differences and other abnormal rhythms [30], and long-term recordings with significant individual differences from a wearable ECG device [31]. The major contributions of the proposed work are summarized below:

1) A new AF detection framework based on DA strategy is proposed to address the limitations of AF detection in wearable ECG monitoring, which enhances AF detection accuracy in dynamic monitoring situations with individual differences and interference from other arrhythmias.
2) Two new AF detectors: DA algorithms based on the Swin-Transformer (DA-ST) and ResNet (DA-RN) are designed to minimize feature distribution differences between annotated ECG databases and unlabeled dynamic ECG recordings, thereby improving the accuracy of AF recognition.
3) The external verification set with other abnormal rhythms is used to verify the proposed method. DA-ST and DA-RN are evaluated on the CPSC2021 database, achieving higher accuracies compared to models without DA. In addition, higher accuracies are also achieved compared to other algorithms, demonstrating their reliability in AF detection.
4) Wearable long-term recordings with significant individual differences are selected as application validation. The proposed method is further validated on 12 wearable long-term recordings, including four premature beats

and four AF with premature beats. The results show high detection accuracies, indicating that the proposed approach can reliably detect AF in dynamic ECG recordings with significant individual differences.

II. Method

A. Database

A DA strategy is used to minimize the feature distribution between the source data (annotated public database) and target data (unlabeled dynamic ECGs). The MIT-BIH AF database was used as the source domain, and four datasets from the 4th China Physiological Signal Challenge (CPSC) 2021 database were used as the target domain. The wearable long-term recordings were used to verify the algorithm.

1) MIT-BIH AF Database: The MIT-BIH AF database obtained from the PhysioNet website (https://www.physionet.org/content/afdb/1.0.0/) [28], [29], comprises 23 AF recordings (21 paroxysmal) with rhythm annotations that include AF, AFL (atrial flutter), J (AV junction rhythm), and N (normal), all sampled at 250 Hz. Each recording has been manually labeled and consists of two ECG channels with a duration of 10 h and 15 min. Lead II is used in this work. We segmented the ECG recordings into 10-s time windows, which were further classified into an AF group (33 450 10-s episode) and a non-AF group (33 450 10-s episode) based on the annotations. Specifically, AFL, J, and N were classified as non-AF.

2) CPSC 2021 Database: The CPSC2021 database, obtained from the 4th CPSC (http://www.icbeb.org/CPSC2021) [30], consists of two public datasets and two test sets (which are not publicly available), all sampled at 200 Hz. The database contains recordings of three rhythm types: paroxysmal AF rhythm (AFp), persistent AF rhythm (AFf), and non-AF rhythm (including normal and other abnormal rhythms). Four datasets were included. The training set I (dataset1) is comprising 153 AF recordings and 481 non-AF recordings from 10 AF patients and 39 non-AF patients. The training set II (dataset2) includes 319 AF recordings and 250 non-AF recordings from 37 AF patients and 14 non-AF patients. The testset I (dataset3) consists of 260 AF recordings and 263 non-AF recordings from 30 AF patients and 10 non-AF patients. The testset I includes ECGs from both the same and different sources as the training set I, with at least one test subset collected using a different ECG monitoring system compared to the training set I. Similarly, testset II corresponds to training set II. The testset II (dataset4) consists of 84 AF recordings and 82 non-AF recordings from 50 AF patients and 18 non-AF patients. In this study, the ECGs from the non-AF group and AFf group were segmented into 10-s episodes (see Table II).

To train the AF detector using a DA strategy, we align 80% of the 10-s episodes from dataset1 and dataset2, respectively. An equal number of AF and non-AF episodes from the MIT-BIH AF database is selected as the source domains using stratified sampling. The dataset3 and dataset4 are used as independent testset of dataset1 and dataset2, respectively.

TABLE II
DETAILS OF CPSC2021 DATABASE

Data	Rhythm types		10-s episode	
	Non-AF	AFf	AF	Non-AF
CPSC2021-dataset 1	481	153	25,996	80,281
CPSC2021-dataset 2	250	319	26,140	24,974
CPSC2021-dataset 3	263	260	21,642	43,664
CPSC2021-dataset 4	82	84	22,875	19,502

TABLE III
DETAILS OF WEARABLE ECG DATABASE

Recording	(10-s episode)	Label
1	17,210	AF
2	15,787	AF
3	15,367	AF, Premature Beat
4	16,006	AF, Premature Beat
5	16,384	AF, Premature Beat
6	11,457	AF, Premature Beat
7	17,717	N
8	16,484	Premature Beat
9	17,436	Premature Beat
10	15,600	Premature Beat
11	16,390	Premature Beat
12	16,902	N

3) Wearable Long-Term ECG Recordings: The wearable long-term ECG recordings, obtained from the wearable ECG device [31], are sampled at 400 Hz and include six AF recordings and six non-AF recordings, all diagnosed by physicians, ranging from 55 to 80 years. In this study, the long-term recordings are segmented into 10-s episodes, of which the details are provided in Table III. The patients are provided informed consent, and the protocol is approved by Jiangsu Provincial People's Hospital.

The first 5000 10-s episodes from each recording are selected for feature distribution alignment, and all the data from each recording are used for testing. For the source domain, 30 000 10-s AF and non-AF episodes are randomly selected from the MIT-BIH AF database.

B. Preprocessing

ECG signals are typically affected by noise interference. To mitigate this, a Butterworth bandpass filter with a passband of 0.5–45 Hz is applied. Additionally, the ECG signals are resampled to 400 Hz.

C. Proposed Method

In order to improve the accuracy of AF detection in wearable ECGs, it is necessary to address the differences in ECG distribution between labeled public databases and unlabeled wearable ECGs. These differences can negatively impact the performance of AF detectors trained on public databases when tested on wearable ECGs. To overcome this limitation, it is imperative to eliminate these distributional differences through appropriate measures. Here, we propose to use domain adaptation techniques to align the feature distributions of the two datasets. This method does not need to manually label the wearable ECGs, and is a suitable method for wearable AF detection, as shown in Fig. 1. We adopt the DAN [27] and

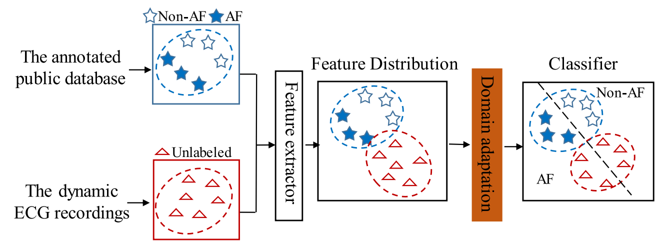

Fig. 1. Domain adaptive framework for detecting AF.

propose two AF detectors: DA-ST and DA-RN to eliminate the difference in ECG feature distribution. In DA-ST AF detector, the DAN is combined with the Swin-Transformer with to detect AF. The DA-RN AF detector adopts a ResNet as the feature extractor for processing ECG data. The network structure of AF detector based on DAN is depicted in Fig. 2.

1) DA Network: The DAN [27] is a transfer learning method and a representative example of domain adaption methods. Its basic structure consists of a feature extractor, a label classifier, and a domain discriminator. The feature extractors for the label classification task and the domain identification task share weights, that is, share the same feature extractor. The network will be trained to enable the label classifier to distinguish the class of data in the source domain, rendering the domain discriminator unable to distinguish the origin of the data. The label classifier and the domain discriminator both include a multilayer perceptron (MLP) and Softmax layer, as shown in Fig. 2. The domain discriminator is inspired by the generative adversarial network (GAN) and is equipped with a gradient reversal layer (GRL), which allows it to effectively align features from the source and target domains. The GRL is placed between the feature extractor and the domain discriminator. During the backpropagation process, the gradient of the domain classification loss of the domain classifier is automatically reversed before backpropagating to the parameters of the feature extractor. This results in the implementation of an adversarial loss, similar to GANs, which further enhances the feature alignment.

The feature extractor is denoted by G_f, the label classifier by G_y, and the domain discriminator is G_d. The loss function L includes two parts [32]: the label classifier loss L_y and the domain discriminator loss L_d, defined as

$$L(\theta_f,\theta_y,\theta_d) = \frac{1}{n}\sum_{x_i \subset D_s} L_y\big(G_y(G_f(x_i)), y_i\big) - \frac{\lambda}{n+m}\sum_{x_i \subset D_s \cup D_t} L_d\big(G_d(G_f(x_i)), d_i\big) \quad (1)$$

where θ_f, θ_y, and θ_d are the parameters of G_f, G_y, and G_d, y_i and d_i are the class label and domain label of a sample x_i, n and m are the of samples in the source and target domains, D_s and D_t denote the datasets of the source and target domains, and λ is a trade-off parameter. θ_f and θ_y are updated by minimizing the loss L to get optimum value $\hat{\theta}_f, \hat{\theta}_y$, while θ_d is updated by maximizing the loss L to get optimum $\hat{\theta}_d$, that is,

$$(\hat{\theta}_f,\hat{\theta}_y) = \arg\min_{\theta_f\theta_y} L(\theta_f,\theta_y,\theta_d) \quad (2)$$

$$(\hat{\theta}_d) = \arg\max_{\theta_d} L(\theta_f,\theta_y,\theta_d). \quad (3)$$

In this work, the cross-entropy loss is used for both the label classifier loss function and domain discriminator loss function.

The stochastic gradient descent (SGD) is used as the optimizer to update θ_f, θ_y, and θ_d, and the initial learning rate μ_0 is set at 0.01. In the DAN, the learning rate is transformed with the iterative process, and the formula is as follows:

$$\mu_p = \frac{\mu_0}{(1+\alpha\cdot p)^\beta} \quad (4)$$

where, μ_0 is the initial learning rate. p represents the relative value of the iteration process, that is, the ratio of the current iteration times to the total iteration times. α and β are hyperparameters. $\alpha = 10$, $\beta = 0.75$.

2) Swin-Transformer: The original transformer architecture often conducts global self-attention operations when processing image data, i.e., calculating the relationships between a token and all other tokens, which can lead to enormous computation and memory costs. Compared with 2-D image data, ECG data are 1-D long sequence data, making the conventional Swin-Transformer unsuitable for AF detection tasks. Here, the latest Swin-Transformer architecture is modified, which greatly reduces the computational memory cost by introducing a shifted window partitioning strategy into the self-attentive module. The shifted 2-D window mechanism of the Swin-Transformer is extended to 1-D windows temporal feature extraction in ECGs.

The feature extraction module of the proposed method is shown in Fig. 2. The input size of the model is (B, 1, 4000), with B the batch size, and the window size is 7. Then after a 4 down the sampling layer, the output dimension is (B, 1000, 32). After that, through three Swin-Transformer blocks and 1/2 down-sampling modules, the output feature dimensions are (B, 500, 64), (B, 250, 128), (B, 125, 256), and (B, 125, 256) respectively. The batch size B was chosen as 64 and the model was trained for 100 epochs.

The standard Swin-Transformer architecture is adopted to make it compatible with the long sequences AF detection tasks. Here, consecutive Swin-Transformer blocks are computed as

$$\hat{z}^l = \text{1DW\_MSA}\big(\text{LN}(\hat{z}^{l-1})\big) + \hat{z}^{l-1} \quad (5)$$

$$z^l = \text{MLP}\big(\text{LN}(\hat{z}^l)\big) + \hat{z}^l \quad (6)$$

$$\hat{z}^{l+1} = \text{1DSW\_MSA}\big(\text{LN}(\hat{z}^l)\big) + \hat{z}^l \quad (7)$$

$$z^{l+1} = \text{MLP}\big(\text{LN}(\hat{z}^{l+1})\big) + \hat{z}^{l+1} \quad (8)$$

where 1DW_MSA and 1DSW_MSA represent window-based multihead self-attention blocks using regular and shifted window configurations, respectively; LN is a LayerNorm layer, $\hat{z}^l$ and z^l denote the output feature of 1DW_MSA and 1DSW_MSA, respectively.

3) Residual Neural Network: The deep neural network based on ResNet architecture is proposed by Ribeiro et al. [26] to diagnose the 12-lead ECG. The input size to the model is

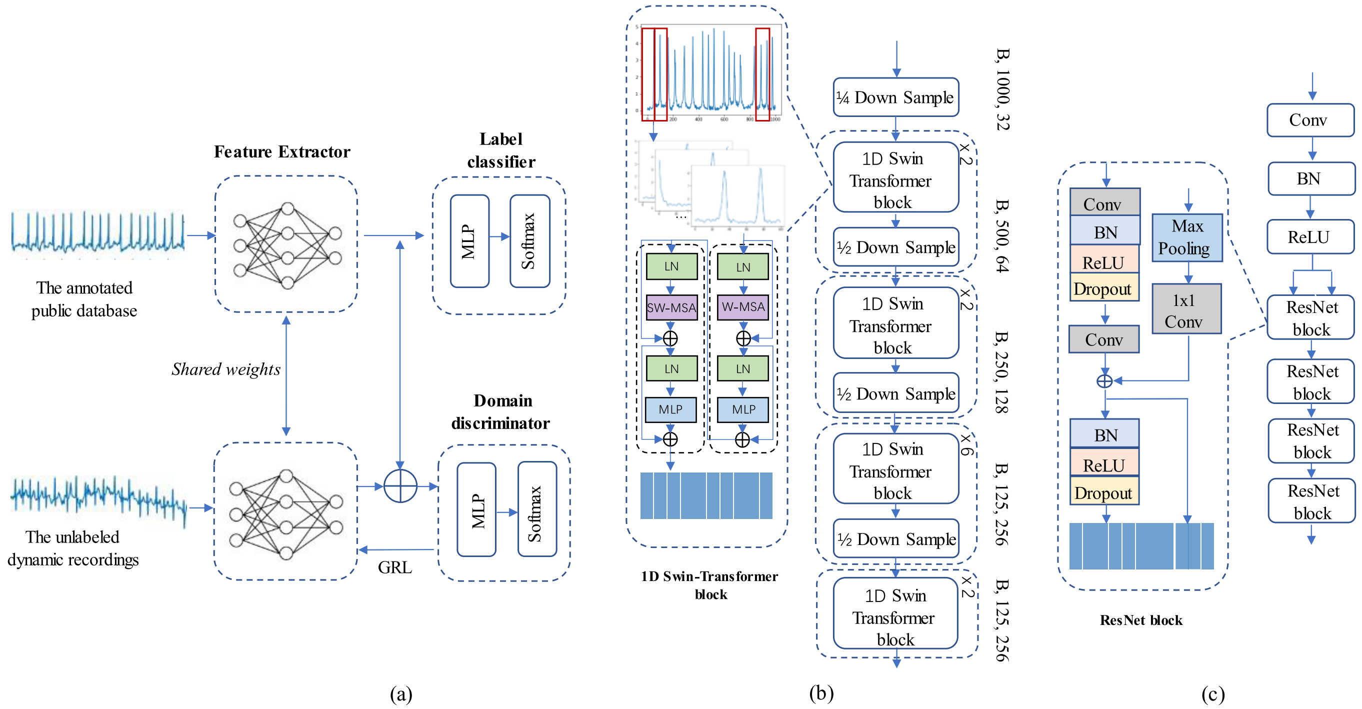

Fig. 2. Architecture of AF detector based on DAN. (a) AF detection network based on DA learning. (b) Feature extractor based on Swin-Transformer. (c) Feature extractor based on ResNet.

originally (12, 4096) in Ribeiro's work. Here, the same deep neural network is applied to single-lead ECG for classifying AF/non-AF signals. The input size is (1, 4000). The model is trained for 60 epochs and the construction of the model is unchanged.

The network included a convolutional layer (Conv) and four ResNet blocks with two Conv per block. Each Conv's output was rescaled by batch normalization (BN), followed by a rectified linear activation unit (ReLU). Dropout is used after ReLU. Skip connections utilize Max Pooling and Conv with a filter length of 1 (1×1 Conv).

The Conv uses a filter length of 16 and begins with 64 filters for the first layer and residual block. The number of filters increases by 64 every second residual block, while subsampling by a factor of 4 occurs at every residual block. The batch size is 32.

D. Experimental Evaluation Methods

Four evaluation indicators are utilized in this study, including Sensitivity (Se), Specificity (Sp), Accuracy (Acc), and Measure of Accuracy (Macc). The four indices used for evaluation are false positive (FP), false negative (FN), true positive (TP), and true negative (TN), which are determined based on the positive or negative labeling of the samples. Where

$$\mathrm{Se} = \mathrm{TP}/(\mathrm{TP}+\mathrm{FN}) \tag{9}$$

$$\mathrm{Sp} = \mathrm{TN}/(\mathrm{TN}+\mathrm{FP}) \tag{10}$$

$$\mathrm{Acc} = (\mathrm{TP}+\mathrm{TN})/(\mathrm{TP}+\mathrm{FN}+\mathrm{TN}+\mathrm{FP}) \tag{11}$$

$$\mathrm{Macc} = (\mathrm{Se}+\mathrm{Sp})/2. \tag{12}$$

The evaluation indicators used for long-term wearable ECG recording are TPt and N, where TPt represents the number of correctly detected 10-s segments in real recordings, and N represents the number of 10-s segments in the long-term recordings. The detection rate is defined as

$$D\_\mathrm{acc} = \mathrm{TPt}/N. \tag{13}$$

III. RESULTS

A. Results From the CPSC 2021 Database

1) Results on Dataset1 and Dataset2: Table IV shows the results on dataset1 and dataset2 when the training set is the MIT-BIH AF database. When using the DA strategy, dataset1 and dataset2 are used as target domain 1 and target domain 2.

For the AF detector based on DA-ST, an increase is observed in the Sp and Se by 12.88% and 11.36% on dataset1 and an increase of 16.55% and 1.67% on dataset2. For AF detector based on DA-RN, the Sp and Se increase by 15.56% and 1.67% on dataset1, and they increase by 17.14% and 5.35% on dataset2.

2) Test Results on Dataset3 and Dataset4: Dataset3 was used as an independent test set for target domain1 and dataset4 is used as an independent test set for target domain2.

Table IV shows the test results on dataset3 and dataset4. DA-ST-based AF detector improves results, with an increase in Sp of 19.57% on dataset3, and an increase in both Sp and Se of 2.79% and 4.42% on dataset4. For the AF detector based on DA-RN, the Sp increases by 22.59% on dataset3 and the Sp and Se increase by 2.81% and 10.44% on dataset4.

TABLE IV
RESULTS ON CPSC2021 DATABASE

Data	Model	*Macc* (%)	*Acc* (%)	*Se* (%)	*Sp* (%)
CPSC2021-dataset1 (Target domian1)	Swin-Transformer	82.51	81.35	84.79	80.23
	ResNet	88.80	84.51	97.20	80.40
	DA-ST	94.63	93.85	96.15	93.11
	DA-RN	97.42	96.67	98.87	95.96
CPSC2021-dataset2 (Target domian2)	Swin-Transformer	80.64	80.84	89.60	71.67
	ResNet	80.85	81.14	93.57	68.13
	DA-ST	89.75	89.78	91.27	88.22
	DA-RN	92.10	92.25	98.92	85.27
CPSC2021-dataset3 （Testset1）	Swin-Transformer	83.39	78.83	96.90	69.87
	ResNet	80.84	75.56	96.48	65.19
	DA-ST	93.19	91.93	96.94	89.44
	DA-RN	92.01	90.58	96.23	87.78
CPSC2021-dataset4 （Testset2）	Swin-Transformer	83.30	83.96	91.62	74.98
	ResNet	82.08	82.54	87.87	76.28
	DA-ST	86.91	87.35	96.04	77.77
	DA-RN	88.70	89.46	98.31	79.09

TABLE V
RESULTS ON THE WEARABLE ECG DATABASE

#Records	Swin-Transformer (%)	DA-ST (%)	ResNet (%)	DA-RN (%)
1	99.65	99.82	98.05	98.87
2	99.73	99.90	99.94	99.99
3	84.62	97.48	98.21	99.26
4	96.97	98.83	98.31	99.34
5	94.07	96.62	98.21	99.91
6	86.28	97.64	98.38	99.89
7	99.65	99.82	96.07	99.88
8	98.62	99.66	96.40	95.79
9	96.08	98.56	79.75	99.85
10	92.19	98.08	88.18	90.14
11	94.09	97.68	86.31	93.61
12	98.82	99.95	94.04	98.25
Average	95.06	98.67	94.32	97.89

B. Results From the Wearable ECG Database

Table V shows the test results on 12 long-term wearable ECG recordings when the MIT-BIH AF database as the training set. The Swin-Transformer-based AF detector achieves an average accuracy of 95.06%, with the best accuracy of 99.73% and the worst accuracy of 84.62% on recording 3. The ResNet-based detector achieves an average accuracy of 94.32%, with the best accuracy of 99.94% and the worst accuracy of 79.75% on Recording 9. In the discussion section, the performance of the Swin-Transformer-based AF detector and ResNet-based AF detector are compared and analyzed in wearable recordings.

The DA-ST-based detector achieves an average accuracy of 98.67%, best accuracy of 99.95%, and worst accuracy of 96.62%. The DA-RN-based detector achieves the best accuracy of 99.99%, the worst accuracy of 90.14%, and an average accuracy of 97.89%.

IV. DISCUSSION

A. Performance Comparison of Algorithms

1) Results Analysis of DA Strategy: The AF detector trained on the MIT-BIH AF database exhibits relatively low accuracy when tested on the CPSC 2021 database. This is because there are significant differences in the data sources between the test set and the training set, as they come from different individuals. The MIT-BIH AF database consists of 23 available AF recordings, while the CPSC 2021 database comprises 127 AF patients and 81 other normal or arrhythmia patients.

A DAN is employed to align the feature distribution of the CPSC 2021 database and the MIT-BIH AF database. The visualization toolkit T-SNE [33] is applied to reduce the features extracted by the feature extractor to 2-D features (Feature1 and Feature2) and draw the feature distribution. Fig. 3 shows the feature distribution before and after using DAN (Swin-Transformer and DA-ST as examples), illustrating the role played by DAN. Meanwhile, the results from DA-ST and DA-RN are equally promising in Tables IV and V, which demonstrate that the DAN can effectively align feature distributions from different data sources, thereby improving the detection accuracy of AF detectors across different individuals.

2) Comparison With Classification Algorithms: Based on the experimental results, it can be observed that Swin-Transformer does not perform as well as ResNet on dataset1 and dataset2. On dataset3 and dataset4, Swin-Transformer performs better than ResNet. For different data, the performance of Swin-Transformer and ResNet is different.

3) Results Analysis of Wearable ECG Recordings: Twelve wearable long-term recordings consist of four premature beats, four AF with premature beats, two sinus rhythms, and two AF, with noticeable interpatient variations. Notably, the MIT-BIH AF database lacks recordings with simultaneous premature beats and AF, and recordings with premature beats.

Fig. 4 shows a comparison of the results from different AF detectors on 12 long-term wearable recordings. The AF detector based on ResNet and the AF detector based on RR interval [22] have a similar ability to detect AF, with relatively high detection rates, but they exhibit a higher false detection rate for other abnormal rhythms, compared to the AF detector based on Swin-Transformer. For AF recordings (Recording 1 and Recording 2) and sinus rhythm recordings (Recording 7 and Recording 12), the AF detectors perform very well. But for AF patients with premature beats (Recording 3 and Recording 6), the AF detector based on Swin-Transformer has a lower accuracy, with test results of only 84.62% and 86.28%, respectively. In contrast, the AF detector based on ResNet performs well. Fig. 5 illustrates examples of 10-s episodes from Recording 3 and Recording 6. Their rhythm information shows up as AF, but the waveform information shows that AF and premature beat occurred simultaneously. Furthermore, for premature beat patients (Recording 8, Recording 9, and Recording 10), the test results from Swin-Transformer exceed 90%, but the test result from ResNet is only 79.95% on Recording 9, and the results for Recording 10 and Recording 11 are 88.18% and 86.31%, respectively. Fig. 5 highlights that the premature atrial contraction (PAC) and ventricular premature contraction (PVC) are from Recording 9 and Recording 11. Their rhythms are similar to that of AF, but the waveforms are not similar. The test results on the wearable database show that Swin-Transformer is more sensitive to waveform information, while ResNet is more sensitive to rhythm information.

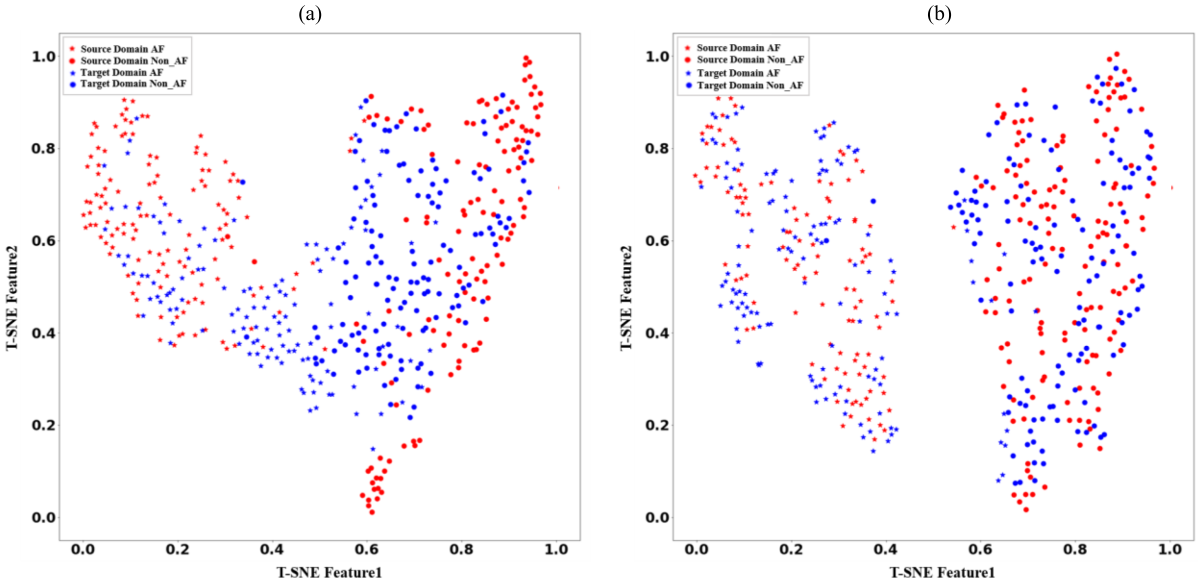

Fig. 3. Feature distributions by T-SNE (Swin-Transformer and DA-ST as examples). (a) Swin-Transformer. (b) DA-ST.

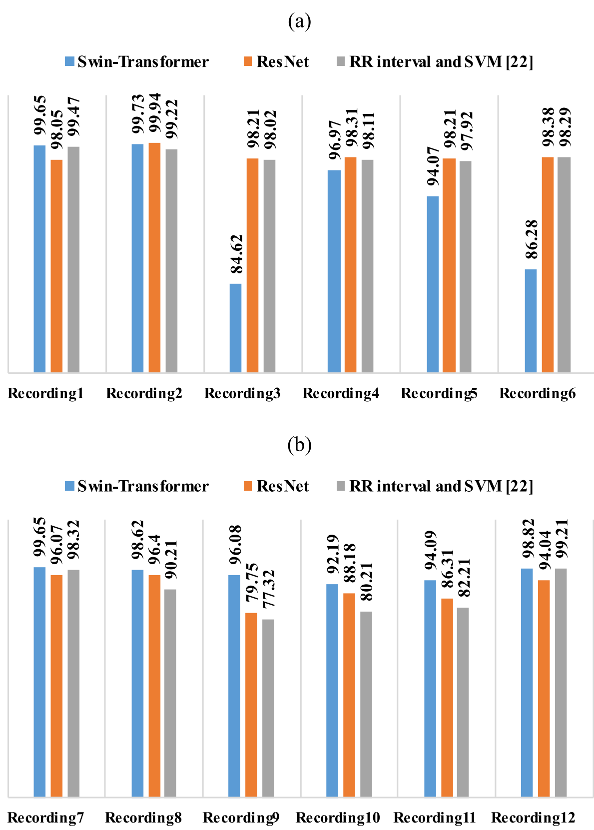

Fig. 4. Comparison of results from different AF detectors on wearable ECG. (a) Comparison of results on AF recordings. (b) Comparison of results on non-AF recordings.

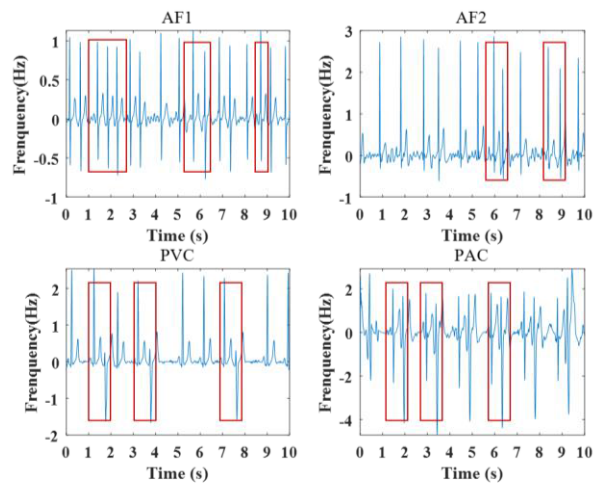

Fig. 5. Examples of 10-s episodes from wearable ECG recordings.

Notably, the significant individual differences and interference with other arrhythmias in the real wearable ECG monitoring state present a challenge for the AF detector. However, aligning the wearable ECG database with the MIT-BIH AF database improves the average test D_acc by 3.61% and 3.57% respectively from DA-ST and DA-RS.

B. Advantages Over Other Algorithm Models

Traditional machine learning-based AF detectors, such as those based on RR interval, have been commonly used for the detection of AF in long-term wearable ECG signals. However, they are prone to misidentifying other arrhythmias as AF. In contrast, deep learning-based AF detectors offer the advantage of end-to-end signal processing. Nonetheless, they face challenges in generalization due to significant waveform differences between individuals and poor performance when tested on independent datasets [22]. In this study, two deep learning-based AF detectors (Swin-Transformer and ResNet) on independent ECG recordings are trained and tested. To address the challenge of personalized differences, a domain adaptive strategy is used, resulting in significantly improved detection accuracy on independent datasets. Table VI shows the performance of the different AF detectors tested on the CPSC2021 database when the MIT-BIH AF database was

TABLE VI
PERFORMANCE OF METHODS ON THE CPSC2021 DATABASE

Test set	Author	Method	*Macc* (%)	*Acc* (%)	*Se* (%)	*Sp* (%)
CPSC2021-dataset1	Vykintas [24]	RR interval feature+LSTM	92.53	92.56	92.47	92.59
	Zhang [23]	LSTM+CNN	83.89	88.44	77.57	90.20
	Shreyasi [35]	Features+Cascaded Binary	91.04	87.88	97.26	84.81
	Morteza [36]	Features+Random Forest	89.11	85.81	95.63	82.59
	Bin [37]	Features +AdaBoost	90.20	90.67	89.25	91.14
	Ma [22]	RR interval features +SVM	93.72	91.75	97.59	89.83
	Ma [34]	LSTM-AE+SVM	97.97	98.24	97.44	98.50
	This work	Swin-Transformer	82.51	81.35	84.79	80.23
	This work	ResNet	88.80	84.51	97.20	80.40
	This work	DA-ST	94.63	93.85	96.15	93.11
	This work	DA-RN	97.42	96.67	98.87	95.96
CPSC2021-dataset2	Vykintas [24]	RR interval feature+LSTM	81.57	81.89	85.38	77.75
	Zhang [23]	LSTM+CNN	79.79	80.96	93.72	65.85
	Shreyasi [35]	Features+Cascaded Binary	82.98	83.99	94.87	71.09
	Morteza [36]	Features+Random Forest	79.41	80.37	90.85	67.96
	Bin [37]	Features+AdaBoost	81.53	81.78	84.57	78.49
	Ma [22]	RR interval features +SVM	87.55	88.28	96.46	78.64
	Ma [34]	LSTM-AE+SVM	91.78	92.14	96.13	87.42
	This work	Swin-Transformer	80.64	80.84	89.60	71.67
	This work	ResNet	80.85	81.14	93.57	68.13
	This work	DA-ST	89.75	89.78	91.27	88.22
	This work	DA-RN	92.10	92.25	98.92	85.27

used as the training set. Compared to AF detectors based on machine learning or deep learning, the DA-ST and DA-RN show better performance.

1) Comparison With Machine Learning Algorithms: Ma et al. [34] evaluated the performance of AF detectors developed by Datta et al. [35], Zabihi et al. [36], Bin et al. [37], and Ma et al. [22] on the dataset1 and dataset2 from CPSC2021 database, and the results are presented in Table VI. The AF detection algorithm from Datta et al. [35] combined AF features and Cascaded Binary, with results on dataset1 of 97.26% for Se and only 84.81% for Sp, and corresponding results on dataset2 of 94.87% and 71.09%. The AF detection algorithm developed by Zabihi et al. [36], which combines AF features and random forest, has a Se of 95.63% and a Sp of 82.59% on dataset1 and 90.85% and 67.96% on dataset2 respectively. Bin et al. [37] developed an AF detection algorithm using AF features and AdaBoost, which achieved Se of 89.25% and Sp of 91.14% on dataset1, corresponding to 84.57% and 78.49% on dataset2. The AF detector developed by Ma et al. [22] achieved the highest performance on the CPSC2021 database, with a Se of 97.59% and Sp of 89.83% on the dataset1, and Se of 96.46% and Sp of 78.64% on the dataset2. However, this AF detector exhibited low detection rate for non-AF. In addition, machine learning-based AF detection algorithms require expert knowledge for feature extraction and feature selection, which is time consuming and complex. DA-ST and DA-RN are end-to-end algorithms and achieve better performance.

2) Comparison With Deep Learning Algorithms: The performance of deep learning-based AF detectors developed by Zhang et al. [23], Maknickas and Maknickas [24], and Ma et al. [34] on the CPSC 2021 database are shown in the Table VI. The AF detector developed by Maknickas and Maknickas [24] achieved a Se of 92.47%, Sp of 92.59% on dataset1, and Se of 85.38%, Sp of 77.75% on dataset2. The AF detector from Zhang et al. [23] had a Sp of 90.20% and a Se of 77.57% on dataset, and a Sp of 65.85% and a Se of 93.72% on dataset2. The AF detector proposed by Ma et al. [34] combined RR interval and P-wave features using LSTM-AE and DTW to detect AF, achieving a Se of 97.44%, Sp of 98.50% on dataset1, and Se of 96.13%, Sp of 87.42% on dataset2. However, this detector required four steps and was combined with SVM and LSTM-AE, resulting in a more complex and time-consuming detection process. On dataset2, DA-RN achieves the best results with no manual intervention.

V. CONCLUSION

To mitigate the impact of individual differences and other abnormal rhythms in dynamic ECG data, we propose improved AF detectors based on Swin-Transformer and ResNet, which utilize a domain adaptation strategy by training on both annotated public databases and unlabeled dynamic ECGs. The proposed method yields improved detection accuracy on independent test data. The proposed detector is evaluated on 12 wearable long-term recordings, including four premature beats, four cases of AF with premature beats, two sinus rhythms, and two cases of AF. The average detection results are 98.67% and 97.89% for the two test sets, respectively. The results demonstrate the potential clinical application of the proposed algorithm. Since the Swin-Transformer introduces a moving window and focuses on localized features, its performance degrades when encountering long sequences of noisy data. In future work, the ECG quality assessment algorithm can be combined with Swin-Transformer for AF detection in wearable ECGs, which will improve the accuracy of AF detection.

REFERENCES

[1] F. Rahman, G. F. Kwan, and E. J. Benjamin, “Global epidemiology of atrial fibrillation,” *Nature Rev. Cardiol.*, vol. 11, no. 11, pp. 639–654, Nov. 2014, doi: 10.1038/nrcardio.2014.118.

[2] J. B. Conti, “Cardiac pacing, defibrillation and resynchronization: A clinical approach,” *Pacing Clin. Electrophysiol.*, vol. 32, no. 8, pp. 1109, Aug. 2009, doi: 10.1111/j.1540-8159.2009.02450.x.

[3] G. Hindricks et al., “2020 ESC guidelines for the diagnosis and management of atrial fibrillation developed in collaboration with the European Association for Cardio-Thoracic Surgery (EACTS),” *Eur. Heart J.*, vol. 42, no. 5, pp. 373–498, Feb. 2021, doi: 10.1093/eurheartj/ehaa612.

[4] J. W. McCready et al., “Predictors of recurrence following radiofrequency ablation for persistent atrial fibrillation,” *Europace*, vol. 13, no. 3, pp. 355–361, Mar. 2011, doi: 10.1093/europace/euq434.

[5] C. Liu, M. Yang, J. Di, Y. Xing, Y. Li, and J. Li, “Wearable ECG: History key technologies and future challenges,” *Chin. J. Biomed. Eng.*, vol. 38, no. 6, pp. 641–652, 2019.

[6] S. Nemati et al., “Monitoring and detecting atrial fibrillation using wearable technology,” in *Proc. 38th Annu. Int. Conf. IEEE Eng. Med. Biol. Soc. (EMBC)*, Aug. 2016, pp. 3394–3397.

[7] Y. Lin, J. Yao, and W. Li, “Clinical analysis of 12-lead Holter on monitoring paroxysmal atrial fibrillation and triggering factor,” *China Modern Med.*, vol. 21, no. 17, p. 3, 2014.

[8] W. C. Choe et al., “A comparison of atrial fibrillation monitoring strategies after cryptogenic stroke (from the cryptogenic stroke and underlying AF Trial),” *Amer. J. Cardiol.*, vol. 116, no. 6, pp. 889–893, Sep. 2015, doi: 10.1016/j.amjcard.2015.06.012.

[9] C. Ma, S. Wei, and C. Liu, “Atrial fibrillation detection in dynamic signals,” in *Feature Engineering and Computational Intelligence in ECG Monitoring*. Cham, Switzerland: Springer, 2020, pp. 177–195.

[10] M. O. Rangel, W. T. O’Neal, and E. Z. Soliman, “Usefulness of the electrocardiographic P-wave axis as a predictor of atrial fibrillation,” *Amer. J. Cardiol.*, vol. 117, no. 1, pp. 100–104, Jan. 2016, doi: 10.1016/j.amjcard.2015.10.013.

[11] D. T. Linker, “Long-term monitoring for detection of atrial brillation,” U.S. Patent 7630 756 B2, Dec. 8, 2009.

[12] C. Liu et al., “A comparison of entropy approaches for AF discrimination,” *Physiolog. Meas.*, vol. 39, no. 7, Jul. 2018, Art. no. 074002, doi: 10.1088/1361-6579/aacc48.

[13] S. Ladavich and B. Ghoraani, “Rate-independent detection of atrial fibrillation by statistical modeling of atrial activity,” *Biomed. Signal Process. Control*, vol. 18, pp. 274–281, Apr. 2015, doi: 10.1016/j.bspc.2015.01.007.

[14] X. Du et al., “A novel method for real-time atrial fibrillation detection in electrocardiograms using multiple parameters,” *Ann. Noninvasive Electrocardiol.*, vol. 19, no. 3, pp. 217–225, May 2014, doi: 10.1111/anec.12111.

[15] R. Alcaraz and J. J. Rieta, “Application of wavelet entropy to predict atrial fibrillation progression from the surface ECG,” *Comput. Math. Methods Med.*, vol. 2012, pp. 1–9, Oct. 2012.

[16] M. García, J. Ródenas, R. Alcaraz, and J. J. Rieta, “Application of the relative wavelet energy to heart rate independent detection of atrial fibrillation,” *Comput. Methods Programs Biomed.*, vol. 131, pp. 157–168, Jul. 2016.

[17] G. D. Clifford et al., “AF classification from a short single lead ECG recording: The PhysioNet/computing in cardiology challenge 2017,” in *Proc. Comput. Cardiol. (CinC)*, Sep. 2017, pp. 1–4, doi: 10.22489/CinC.2017.065-469.

[18] K. Luo, J. Li, Z. Wang, and A. Cuschieri, “Patient-specific deep architectural model for ECG classification,” *J. Healthcare Eng.*, vol. 2017, pp. 1–13, May 2017, doi: 10.1155/2017/4108720.

[19] Y. Zhang, Y. Huang, K. Wang, and C. Liu, “Arrhythmia classification using parallel combination of LSTM and CNN,” *J Harbin Inst. Technol*, vol. 51, no. 10, pp. 76–82, 2019.

[20] R. S. Andersen, A. Peimankar, and S. Puthusserypady, “A deep learning approach for real-time detection of atrial fibrillation,” *Expert Syst. Appl.*, vol. 115, pp. 465–473, Jan. 2019, doi: 10.1016/j.eswa.2018.08.011.

[21] Y.-C. Chang, S.-H. Wu, L.-M. Tseng, H.-L. Chao, and C.-H. Ko, “AF detection by exploiting the spectral and temporal characteristics of ECG signals with the LSTM model,” in *Proc. Comput. Cardiol. Conf. (CinC)*, vol. 45, Sep. 2018, pp. 1–4.

[22] C. Ma, S. Wei, T. Chen, J. Zhong, Z. Liu, and C. Liu, “Integration of results from convolutional neural network in a support vector machine for the detection of atrial fibrillation,” *IEEE Trans. Instrum. Meas.*, vol. 70, pp. 1–10, 2021, doi: 10.1109/TIM.2020.3044718.

[23] X. Zhang, J. Li, Z. Cai, L. Zhang, Z. Chen, and C. Liu, “Over-fitting suppression training strategies for deep learning-based atrial fibrillation detection,” *Med. Biol. Eng. Comput.*, vol. 59, no. 1, pp. 165–173, Jan. 2021, doi: 10.1007/s11517-020-02292-9.

[24] V. Maknickas and A. Maknickas, “Atrial fibrillation classification using QRS complex features and LSTM,” in *Proc. Comput. Cardiol. (CinC)*, Sep. 2017, pp. 1–4.

[25] Z. Liu et al., “Swin transformer: Hierarchical vision transformer using shifted windows,” in *Proc. IEEE/CVF Int. Conf. Comput. Vis. (ICCV)*, Oct. 2021, pp. 9992–10002.

[26] A. H. Ribeiro et al., “Automatic diagnosis of the 12-lead ECG using a deep neural network,” *Nature Commun.*, vol. 11, no. 1, p. 1760, Apr. 2020, doi: 10.1038/s41467-020-15432-4.

[27] Y. Ganin et al., “Domain-adversarial training of neural networks,” *J. Mach. Learn. Res.*, vol. 17, no. 1, pp. 2030–2096, Apr. 2016, doi: 10.1007/978-3-319-58347-1_10.

[28] G. Moody, “A new method for detecting atrial fibrillation using R-R intervals,” *Comput. Cardiol.*, vol. 10, pp. 227–230, Jan. 1983.

[29] A. L. Goldberger et al., “PhysioBank, PhysioToolkit, and PhysioNet: Components of a new research resource for complex physiologic signals,” *Circulation*, vol. 101, no. 23, pp. E215–E220, Jun. 2000.

[30] X. Wang, C. Ma, X. Zhang, H. Gao, G. Clifford, and C. Liu, “Paroxysmal atrial fibrillation events detection from dynamic ECG recordings: The 4th China physiological signal challenge,” in *PhysioNet*, 2021. [Online]. Available: https://doi.org/10.13026/ksya-qw89

[31] C. Liu et al., “Signal quality assessment and lightweight QRS detection for wearable ECG SmartVest system,” *IEEE Internet Things J.*, vol. 6, no. 2, pp. 1363–1374, Apr. 2019, doi: 10.1109/JIOT.2018.2844090.

[32] H. Ren, J. Wang, J. Dai, Z. Zhu, and J. Liu, “Dynamic balanced domain-adversarial networks for cross-domain fault diagnosis of train bearings,” *IEEE Trans. Instrum. Meas.*, vol. 71, pp. 1–12, 2022.

[33] L. Van der Maaten and G. Hinton, “Visualizing data using t-SNE,” *J. Mach. Learn. Res.*, vol. 9, no. 11, pp. 1–27, 2008.

[34] C. Ma et al., “A multistep paroxysmal atrial fibrillation scanning strategy in long-term ECGs,” *IEEE Trans. Instrum. Meas.*, vol. 71, pp. 1–10, 2022, doi: 10.1109/TIM.2022.3164138.

[35] S. Datta et al., “Identifying normal, AF and other abnormal ECG rhythms using a cascaded binary classifier,” in *Proc. Comput. Cardiol. (CinC)*, Sep. 2017, pp. 1–4, doi: 10.22489/CinC.2017.173-154.

[36] M. Zabihi, A. B. Rad, A. K. Katsaggelos, S. Kiranyaz, S. Narkilahti, and M. Gabbouj, “Detection of atrial fibrillation in ECG hand-held devices using a random forest classifier,” in *Proc. Comput. Cardiol. (CinC)*, Sep. 2017, pp. 1–4, doi: 10.22489/CinC.2017.069-336.

[37] G. Bin, M. Shao, G. Bin, J. Huang, D. Zheng, and S. Wu, “Detection of atrial fibrillation using decision tree ensemble,” in *Proc. Comput. Cardiol. (CinC)*, Sep. 2017, pp. 1–4, doi: 10.22489/CinC.2017.342-204.

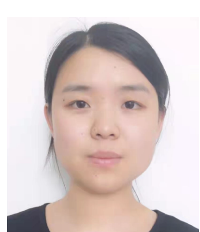

Caiyun Ma (Graduate Student Member, IEEE) received the M.S. degree in biomedical engineering from Shandong University, Jinan, China, in 2020. She is currently pursuing the Ph.D. degree in instrument science and technology from Southeast University, where she mainly works on physiological signals processing and the atrial fibrillation signals classification using machine learning.

Xi Long (Senior Member, IEEE) was born in China, in 1983. He received the B.Eng. degree (Hons.) in electronic information engineering from Zhejiang University, Hangzhou, China, in 2006, and the M.Sc. and Ph.D. (cum laude) degrees in electrical engineering from the Eindhoven University of Technology, Eindhoven, The Netherlands, in 2009 and 2015, respectively.

From 2010 to 2011, he was with Tencent, Shenzhen, China, working on data mining and user research. He has more than ten years of research and development experience in healthcare industry, with Philips Research, Eindhoven, The Netherlands, where he has been a Senior Scientist and an AI Lead. He is currently an Associate Professor with the Signal Processing Systems Group, Department of Electrical Engineering, Eindhoven University of Technology. He has published over 120 articles and reports in these fields and his inventions led to more than 15 patent applications. His research interests include signal processing and machine learning in healthcare and medical applications.

Weijie Sheng received the M.S. degree in marine engineering from the Huazhong University of Science and Technology, Wuhan, China, in 2013, and the Ph.D. degree in control science and engineering from Southeast University, Nanjing, China, in 2022.

He is currently with the School of Information Engineering, Yangzhou University, Yangzhou, China, where he mainly works on pattern recognition, computer vision, biometric techniques, gait-based identity recognition, gait-based emotion recognition, machine learning algorithms, and deep learning networks.

Rik Vullings (Senior Member, IEEE) received the M.Sc. degree in applied physics and the Ph.D. degree in electrical engineering from the Eindhoven University of Technology (TU/e), Eindhoven, The Netherlands, in 2005 and 2010, respectively.

He is currently an Associate Professor with the Biomedical Diagnostics Laboratory, Signal Processing Systems Group, Department of Electrical Engineering, TU/e. His main research interests include probabilistic model driven and data driven signal processing techniques for biomedical applications.

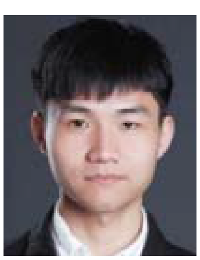

Meicheng Yang received the B.S. degree in measurement and control technology and instrumentation from Zhengzhou University, Zhengzhou, China, in 2018. He is currently pursuing the Ph.D. degree in instrument science and technology with Southeast University, Nanjing, China, where he mainly working on physiological signals processing, machine learning in healthcare, and intelligent clinical decision systems.

Lina Zhao received the B.S. and M.S. degrees in biomedical engineering from Shandong University, Jinan, China, in 2005 and 2008, respectively, where she is currently pursuing the Ph.D. degree with the School of Control Science and Engineering.

She is currently receiving a post-doctoral trainings with Southeast University, Nanjing, China. Her current research interests include entropy methods for physiological signal analysis, electrocardiogram, PCG, and artery pressure pulse processing.

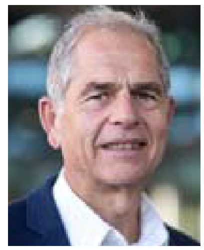

Ronald M. Aarts (Fellow, IEEE) was born in Amsterdam, The Netherlands, in 1956. He received the B.S. degree in EE and the Ph.D. degree in physics from the Delft University of Technology, Delft, The Netherlands, in 1977 and 1995, respectively.

He joined Philips Research Labs, Eindhoven, The Netherlands, in 1977. He has been a part-time Full Professor with the Eindhoven University of Technology, Eindhoven, since 2006, where he is mainly involved in supervising the master's and Ph.D. students. He has been the President of Aarts Consultancy, since 1990. He has published over 450 articles and reports and holds over 110 granted U.S.-patents. His research interests include acoustics and engineering to medicine and biology in particular sensors, signal processing, systems for ambulatory and unobtrusive-monitoring, sleep, cardiology, perinatal, drugs response monitoring (DRM), and epilepsy detection.

Jianqing Li received the B.S. and M.S. degrees in automatic technology from the School of Instrument Science and Engineering, Southeast University, Nanjing, China, in 1986 and 1992, respectively, and the Ph.D. degree in measurement technology and instruments from Southeast University.

He is currently a Professor and the Vice President with the School of Basic Medical Sciences, Nanjing Medical University, Nanjing. He is also a Professor with the School of Instrument Science and Engineering, Southeast University. His research interests include mHealth and wireless networks.

Chengyu Liu (Senior Member, IEEE) received the Ph.D. degree in biomedical engineering from Shandong University, Jinan, China, in 2010.

He completed post-doctoral training with Shandong University, from 2010 to 2013; Newcastle University, Newcastle upon Tyne, U.K., from 2013 to 2014; and Emory University, Atlanta, GA, USA from 2015 to 2017. He is currently the Director and a Professor with the Southeast-Lenovo Wearable Heart-Sleep-Emotion Intelligent Monitoring Laboratory, School of Instrument Science and Engineering, Southeast University, Nanjing, China. He has published more than 180 articles, including more than 80 SCI journal articles and eight chapters in books, and has more than ten invention patents. His main research interests include intelligent monitoring and analysis of vital signs signals (ECG, blood pressure, pulse, respiration, and heart sounds), medical big data processing and machine learning, research, and development of wearable active health monitoring device.

Dr. Liu is currently a Federation Journal Committee Member of the International Federation for Medical and Biological Engineering (IFMBE).